Molecular Catalysis 462 (2019) 114–125

Contents lists available at ScienceDirect

Molecular Catalysis

journal homepage: www.elsevier.com/locate/mcat

Aminoiron(III)–porphyrin–alumina catalyst obtained by non-hydrolytic sol-gel process for heterogeneous oxidation of hydrocarbons

Michelle Saltarelli[a], Emerson H. de Faria[a], Katia J. Ciuffi[a,*], Eduardo J. Nassar[a,*], Raquel Trujillano[b], Vicente Rives[b], Miguel A. Vicente[b]

[a] Universidade de Franca, Av. Dr. Armando Salles Oliveira 201 – Pq. Universitário, 14404-600 Franca, SP, Brazil
[b] GIR-QUESCAT, Departamento de Química Inorgánica, Facultad de Ciencias Químicas, Universidad de Salamanca, 37008 Salamanca, Spain

ARTICLE INFO

Keywords:
Alumina
Immobilization
Aminoiron(III) porphyrin
Sol-gel process
Heterogeneous oxidation catalysis

ABSTRACT

An aminoiron(III) porphyrin immobilized on an alumina matrix was prepared and used as catalyst for the oxidation of organic substrates. Powder alumina had been prepared by a non-hydrolytic sol-gel method through condensation of aluminum chloride with anhydrous ethanol. Then, iron(III) [5,10,15,20-tetrakis(2,6-dichloro-3-aminophenyl)-porphyrin] was immobilized on the alumina powder under magnetic stirring, reflux, and inert atmosphere. Ultraviolet–visible and infrared spectroscopies, powder X-ray diffraction, scanning electron microscopy and thermal analysis were applied for characterizing the resulting material, confirming that the ironporphyrin was immobilized on the alumina support. The catalytic activity of ironporphyrin/alumina was evaluated in the oxidation of (*Z*)-cyclooctene and cyclohexane and in the Baeyer-Villiger oxidation of cyclohexanone using iodosylbenzene or hydrogen peroxide as oxygen donors. The novel immobilized catalyst proved to be a promising system for the efficient and selective oxidation of the organic substrates with 85–92% selectivity to the epoxide in the oxidation of alkenes and 25–41% to the ketone in the oxidation of cyclohexane. As for the Baeyer-Villiger oxidation of cyclohexanone, good conversion to ε-caprolactone was observed as well. The material is a reusable heterogeneous catalyst, which makes it more economically feasible than its homogeneous counterpart.

1. Introduction

The development of environmentally friendly and economically viable processes to obtain fine chemicals is certainly one of the greatest challenges that humankind has to face to ensure sustainable growth on our planet [1]. Catalysis is a science that substantially contributes to meeting this challenge: it promotes sustainability, preserves the environment, saves energy, and improves health conditions and quality of life [2].

Inspired by effective biological oxidation systems, several authors have attempted in recent years to develop efficient, selective, accessible, low-cost, and reusable biomimetic catalysts to oxidize organic molecules under mild conditions [2–5]. The family of cytochrome P-450 monooxygenases has attracted much interest for over 50 years, as these enzymes can use molecular oxygen (O_2) to oxidize organic substrates generating water as a byproduct: they insert an oxygen atom into the substrate while the other oxygen atom is used to generate water. In addition, these monooxygenases are key to the oxidative metabolism of drugs and xenobiotics in living organisms [6]. However, comparison between cytochrome P-450 models like metalloporphyrins (MePs) and the enzyme itself reveals significant differences. First, the enzyme bears a protein matrix that isolates ironprotoporphyrin IX, the active site that catalyzes the oxidation reactions, controls the reactivity of the oxidant, and prevents the enzyme from being inactivated. This protein matrix also provides a hydrophobic environment favoring the bonding between the substrate and the active site and controlling the accessibility of the substrate to the active species, thereby increasing the selectivity of the oxidation [7].

The use of MePs in homogeneous medium in an industrial setting possess difficulties, namely, its recovery, reuse, and high cost of the catalyst as well as the dimerization and oxidative self-destruction of MePs [8]. These issues have been mitigated by strategies such as the synthesis of heterogeneous organic-inorganic catalysts and the immobilization of MePs on different materials like silica [9], clays [10], alumina [11] and MOFs [12], among other supports. Encapsulated catalysts are advantageous because they promote the control of the reaction medium and conditions, prevent the chemical degradation of the catalyst, enable cost-effective catalyst recycling, and enhance the

* Corresponding authors.
E-mail addresses: katia.ciuffi@unifran.edu.br (K.J. Ciuffi), eduardo.nassar@unifran.edu.br (E.J. Nassar).

https://doi.org/10.1016/j.mcat.2018.09.014
Received 27 July 2018; Received in revised form 11 September 2018; Accepted 17 September 2018
Available online 08 October 2018
2468-8231/

stability of the catalyst. Selective catalytic materials may result from the controlled formation of either a pore structure or a solid three-dimensional network [12,13].

Sol-gel processes have opened promising possibilities to prepare hybrid organic–inorganic advanced materials containing MePs entrapped into matrixes to catalyze oxidation reactions. The sol-gel process offers the best experimental conditions to obtain silica [3,12] as a solid matrix for MePs. Amorphous aluminosilicates [8] and aluminum oxide (alumina) [11] can also be used to immobilize MePs.

The hydrolytic sol-gel (HSG) route consists of two steps: (1) hydroxylation of the inorganic or organic-metal precursor, and (2) condensation of the hydroxyl groups in the presence of an acid or basic catalyst. However, the HSG route requires water as solvent, a medium where controlling the microstructure of the oxide is difficult [14,15]. Therefore, much work has been recently focused on the non-hydrolytic sol-gel (NHSG) [16–19] route.

Most of the reactions reported in the literature to obtain materials by the NHSG route for application in catalysis are based on the condensation of a metal or semi-metal alkoxide with a metal or semi-metal halide, to yield an oxide under non-aqueous conditions. The NHSG route has many advantages, as the alkoxide originates *in situ* by reaction of the metal halide with ethers or alcohols, which reduces the reaction costs and facilitates the synthetic process [19].

We have previously reported on the synthesis of MePs encapsulated in amorphous networks of alumina and derivatives by the NHSG route [11,20,21]. This route has also been used to prepare efficient catalysts based on metal complexes and Jacobsen catalysts. Table 1 lists selected catalytic materials that have been synthesized by NHSG routes. The non-hydrolytic route was fundamental for the feasible functionalization of these complexes, allowing the construction of more active catalysts, avoiding their destruction under the conditions of the reaction, and preventing dimerization or leaching of the catalyst.

In an attempt to develop a heterogeneous catalyst, inspired by biological systems, to increase efficiency, selectivity and catalytic reuse, in the present paper amorphous alumina has been prepared by the NHSG process. Alumina is a porous solid and finds applications mainly as adsorbent, catalyst and catalyst support. Based on the experience in our research group with the non-hydrolytic sol-gel method [11,20,21,25], it is believed that, even with so many advantages, it can still be improved mainly as a promising route using environmentally friendlier solvent (ethanol) and oxidant (H_2O_2). Sol-gel processing of alumina has created novel applications and has improved some of its properties [11]; thereby, the ethanol route was used. The resulting alumina was used to immobilize a MeP, namely a FeP, of catalytic interest. The immobilized MeP/alumina catalyst was applied in green oxidation reactions, namely the epoxidation of (*Z*)-cyclooctene, the ketonization of cyclohexane, and the Baeyer-Villiger (BV) oxidation of cyclohexanone.

2. Experimental

Analytical grade chemicals were purchased from Aldrich, Sigma, or Merck, and were used without any further treatment.

Iodosylbenzene (PhIO) was synthesized by hydrolysis of iodosylbenzene diacetate according to the method described by Sharefkin and Saltzman [27]. The purity of PhIO (98%) was determined by titration with sodium thiosulfate in the presence of starch as indicator.

The anhydrous solution of hydrogen peroxide (H_2O_2, 24 wt.%) in ethyl acetate was prepared by azeotropic distillation as described previously by Stefen et al. [28]. An aqueous solution of H_2O_2 was used as the starting material to prepare the anhydrous solution of H_2O_2. The azeotropic distillation was carried out in a system where the oxygen generated by decomposition of H_2O_2 was released to the atmosphere. The aqueous solution of H_2O_2 was kindly supplied by Peróxidos do Brasil S.A. and was standardized by permanganometric titration.

The purity of the substrates (*Z*)-cyclooctene, cyclohexane, and cyclohexanone was determined by gas chromatography. (*Z*)-cyclooctene was purified by column chromatography on basic alumina immediately prior to use.

To obtain iron(III) [5,10,15,20-tetrakis(2,6-dichloro-3-aminophenyl)-porphyrin], [FeP], 5,10,15,20-tetrakis(2,6-dichloro-3-nitrophenyl)porphyrin ($H_2TDC(NO_2)P$) was first synthesized as previously described by Oliveira et al. [29] following the method described by Lindsey [30]. Briefly, 7.5 g (0.35 mmol) of 2,6-dichloro-3-nitrobenzaldehyde, 2.4 mL (35.0 mmol) of pyrrole, and 0.5 mL of $BF_3{\cdot}Et_2O$ (1.4 mmol) were reacted, and the resulting porphyrinogen was oxidized by addition of 5.7 g of tetrachloro-1,4-benzoquinone (p-chloranil) (33.0 mmol) in 400 mL of toluene. The crude product was first purified by column chromatography on alumina, using dichloromethane (DCM) as eluent. Then, the resulting porphyrin was purified again by column chromatography on silica gel, using DCM as eluent. After re-crystallization from a DCM/cyclohexane mixture, the desired product was obtained in 26% yield (UV–vis (DCM), λ_{max} = 418 (Soret band), 512, 588 nm).

To obtain 5,10,15,20-tetrakis(2,6-dichloro-3-aminophenyl)porphyrin ($H_2TDC(NH_2)P$), the nitro groups of $H_2TDC(NO_2)P$ were reduced. To this end, 1.1 g (1.1 mmol) of $H_2TDC(NO_2)P$ was dissolved in 70.0 mL of HCl containing 4.1 g (18.2 mmol) of $SnCl_2.H_2O$. The solution was stirred at 70 °C for 1 h. After cooling in an ice bath, the solution was neutralized with ammonia and stirred at 20 °C for 12 h. The solvent was removed under vacuum, and the solid residue was extracted with acetone, to afford $H_2TDC(NH_2)P$ in 95% yield (UV–Vis (DCM), (λ_{max} = 416 (Soret band), 512, 589 nm).

Metal insertion into $H_2TDC(NH_2)P$ was performed as described by Adler and Longo [31]. $H_2TDC(NH_2)P$ was refluxed with iron(II) chloride in dimethylformamide (DMF), which was then removed under vacuum. FeP was washed with water to remove iron salts in excess. This procedure afforded MeP in 80% yield (UV–Vis (acetone), λ_{max} = 369, 419 (Soret band), 508, 655 nm).

The immobilized catalyst was prepared by the NHSG alcohol route adapting the previous methods [11,32,33]. An amount of 7.5 g of anhydrous aluminum chloride ($AlCl_3$) was dissolved in 30.0 mL of anhydrous ethanol (EtOH – oxygen donor and solvent) in a three-neck flask, and kept under magnetic stirring for 10 min. A solution prepared with 52.012 mg (0.0469 mmol) of FeP and 30.0 mL of EtOH was then added to the flask. The reaction solution was refluxed in argon at 110 ± 10 °C

Table 1
Catalysts and photocatalysts prepared by the non-hydrolytic sol-gel (NHSG) route.

Material	Route/precursors	Reaction	Reference
Fe–Al	Ether route: $AlCl_3$, $FeCl_3$, iPr_2O	Mild oxidation with hydrogen peroxide	[21]
Co–Al	Ether route: $AlCl_3$, $CoCl_2$, iPr_2O	Epoxidation of olefin with iodosylbenzene	[22]
Co–Si–Al	Ether route: $SiCl_4$, $AlCl_3$, $CoCl_2$, iPr_2O	Mild oxidation with iodosylbenzene	[20]
Ti–Si	Ether route: $SiCl_4$, $TiCl_4$, iPr_2O	Mild oxidation with hydrogen peroxide	[23]
TiO_2	Benzyl alcohol route: $TiCl_4$ in benzyl alcohol	Photo-oxidation	[24]
Jacobsen catalyst entrapped into Al_2O_3	Ether route: $AlCl_3$, iPr_2O, Mn- or Fe-salen complexes	Selective oxidation with various oxidants	[25]
MePs entrapped into Al_2O_3	Ether route: $AlCl_3$, iPr_2O, MeP	Epoxidation with iodosylbenzene	[26]

for 4 h. The obtained gel was cooled and aged in the reaction medium at room temperature for 24 h. After that the solvent was removed under vacuum, and a final drying step was carried out at 70 °C. The dry gel was then washed with EtOH/water, filtered, and submitted to heat treatment at 100 °C. The final material was designated Al-FeP. Iron was not detected in the mother liquors, indicating that all the ironporphyrin was retained by the alumina formed, leading to a concentration of 9.62 mg of ironporphyrin per gram of alumina. An alumina blank, designated Al_2O_3, was also synthesized by the same procedure, but in the absence of MeP.

To study the oxidation of (Z)-cyclooctene by PhIO, 10 mg of Al-FeP, 5 mg of PhIO, 150 μL of (Z)-cyclooctene (previously purified on alumina column), 1000 μL of a dichloroethane (DCE)/acetonitrile (ACN) mixture (1:1 v/v), and 10 μL of di-*n*-butyl ether as internal standard were added to a 2-mL vial sealed with a Teflon-coated silicone septum. The mixtures were kept under magnetic stirring at room temperature (~27 °C). The catalyst/substrate/oxidant molar ratio was 1:1000:2000, and molar ratios of 1:2000:2000 and 1:1000:4000 were also tested. When H_2O_2 was used as an oxidant, different relative concentrations of the oxidant were used. More specifically, oxidation of (Z)-cyclooctene was first carried out with 220 μL of anhydrous H_2O_2, 20 mg of Al-FeP, 80 μL of (Z)-cyclooctene, 961 μL of a DCE/ACN mixture (1:1 v/v), and 6 μL of di-*n*-butyl ether as internal standard. Oxidation reactions with 70% wt. H_2O_2 as oxidant were also accomplished; the same proportions described above were used, except for the oxidant (130 μL) and the solvent (1114 μL). All the reactants were added to a 2-mL vial sealed with a Teflon-coated silicone septum. The tests were accomplished at room temperature (~27 °C) or 55 °C, and the catalyst/substrate/oxidant molar ratio was 1:3000:1500. In the same way, the tests performed to the supernatant solutions, before and after the reaction, did not detect catalytic activity of the materials and this ruled out the presence of any active metal for catalysis. It is also important to note that the UV–vis spectra did not show in any case the de-metallization of ironporphyrin, ruling out the presence of iron species.

The Al-FeP sample was tested as a catalyst in the oxidation of a saturated hydrocarbon, namely cyclohexane. When PhIO was used as oxidant, the conditions were the same as those described above for the oxidation of (Z)-cyclooctene by PhIO. When H_2O_2 was the oxidant, different relative concentrations of the oxidant were used: oxidation of cyclohexane was carried out by using 220 μL of anhydrous H_2O_2, 20 mg of Al-FeP, 60 μL of cyclohexane, 981 μL of a DCE/ACN mixture (1:1 v/v), and 6 μL of di-*n*-butyl ether as internal standard. When H_2O_2 70 wt.% was used as oxidant, the same proportions were used, except for the oxidant (130 μL) and the solvent (1134 μL). All the reactants were added to a 2-mL vial sealed with a Teflon-coated silicone septum. The tests were accomplished at room temperature (~27 °C) and 55 °C. The catalyst/substrate/oxidant molar ratio was 1:3000:1500.

To study the catalysis under homogeneous conditions, the amount of catalyst was 0.2 mg (the same as it was calculated to be on the support).

The Baeyer – Villiger oxidation reaction was carried out in a 4.0 mL glass reactor. For this reaction, 60 μL of cyclohexanone, 1134 μL of benzonitrile, 6 μL of di-*n*-butyl ether, 220 μL of anhydrous H_2O_2, and 20 mg of Al-FeP were added to the reactor. When 70 wt.% H_2O_2 was used as oxidant, the same proportions were used, except for the oxidant (130 μL) and the solvent (1114 μL). The tests were accomplished at room temperature (~27 °C) and 55 °C. The catalyst/substrate/oxidant molar ratio was 1:3000:1500.

The products of the oxidation reactions were analyzed by gas chromatography at different times of injection (at 2, 4, 24, and 48 h after the reaction started). The yields were determined by comparison with a high purity commercial reagent samples and by using calibration curves. At the end of the oxidation of (Z)-cyclooctene with anhydrous H_2O_2 as oxidant, Al-FeP was recovered by centrifugation, washed five times with methanol (1 mL), dried at 70 °C for 24 h, and reused under the same conditions as in the initial oxidation reaction.

To study the mechanisms involved in the oxidation of (Z)-cyclooctene and cyclohexane, the reactions that provided the best results were repeated in the presence of the well known radical trap scavenger hydroquinone (HQ); this was added at a 1:1 oxidant/HQ molar ratio. The reactions were monitored by gas chromatography for 48 h.

To investigate the acidity of the materials, the samples previously dried in a vacuum oven at 80 °C for 24 h were pressed into self-supporting wafers and placed in an infrared cell under vacuum for 2 h at room temperature for adsorption of pyridine. Subsequently, the FTIR spectra were recorded. The Brönsted and Lewis acid contents, q_H and q_L (μmol g^{-1}), were calculated with the equation [34]:

$$q_{H,L} = (A_I \pi D^2)\ (4w\epsilon_I)^{-1} \quad (1)$$

where D (cm) is the diameter of the wafer, and w (g) the sample weight. The integrated areas A_I (in arbitrary units) of the bands at 1535 (Py-B), 1485 (Py-B/Py-L) and 1450 cm^{-1} (Py-L) were provided by the software of the instrument, after baseline optimization. The extinction coefficients ϵ_I of the bands originated by pyridine interacting with Brønsted and Lewis sites given by Emeis [35], 1.67 ± 0.12 cm $mmol^{-1}$ and 2.22 ± 0.21 cm $mmol^{-1}$, respectively, were used.

The powder X-ray diffraction (PXRD) patterns of non-oriented powder samples were obtained on a Siemens D-500 diffractometer with Ni-filtered Cu Kα radiation, at 40 kV and 30 mA, at a scanning rate of 2°(2θ) min^{-1}.

The Fourier-transform infrared (FTIR) spectra were recorded in the 4000–350 cm^{-1} range on a Perkin-Elmer Spectrum-One spectrometer. The KBr pellet technique was used. About 1 mg of the sample and 300 mg of KBr were mixed to prepare the pellets.

Thermogravimetric analysis (TG) and differential thermal analysis (DTA) were carried out on a Thermal Analysis TA Instruments SDT Q600, from 25 to 1000 °C, under oxygen flow (30 mL min^{-1}), at a heating rate of 20 °C min^{-1}.

The ultraviolet–visible (UV–vis) spectra of the solids in DCM were recorded on a Hewlett-Packard 8453, Diode Array UV–vis spectrophotometer. The samples were placed in an optical cell with a path length of 2.0 mm. DCM was selected as a solvent because it led to improved UV–vis spectra when the suspension was prepared.

The specific surface areas (S_{BET}) were determined by applying the BET method to the corresponding nitrogen adsorption isotherms, recorded in a Micrometrics ASAP 2020 physical adsorption analyzer. The samples were previously degassed for 1 h at room temperature, at a pressure lower than 50 μmHg. The nitrogen adsorption data were obtained using 0.2 g of the sample.

The cationic exchange capacity (CEC) of the materials was calculated by adsorption of methylene blue (MB), as previously detailed by us [36], which also allowed to calculate the total surface area accessible to this molecule (SSA).

For scanning electron microscopy (SEM) images, a VEGA 3 SBH - EasyProbe model, TESCAN, was used. The samples were first coated with a thin gold film.

The reaction products were analyzed by gas chromatography (GC) on an HP 6890 chromatograph equipped with a hydrogen flame ionization detector and capillary column (HPINNOWax-19091 N-133, polyethylene glycol, length = 30 m, internal diameter = 0.25 mm). Quantification was carried out by using a calibration curve obtained with a standard solution, and the yields were based on the added PhIO or on the conversion of the substrate when H_2O_2 was used as oxidant, given as percentage (mol product/mol substrate × 100).

3. Results and discussion

Our group has previously reported the use of ether-based NHSG route to remove alkyl halides in the preparation of inorganic oxide-based materials such as alumina [22,21], aluminosilicate [20], titanosilicate [37] and titania [38]. In all these cases, the reactions were

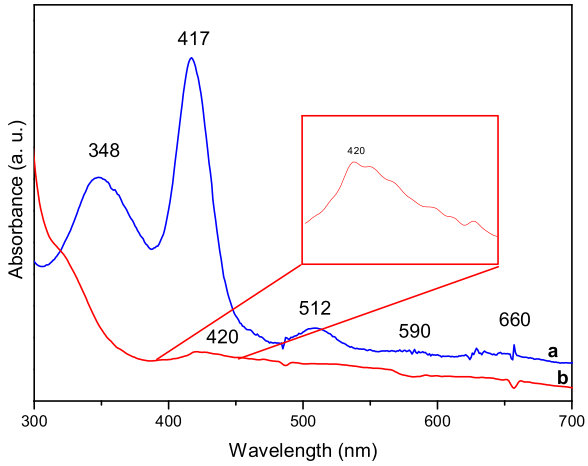

Fig. 1. UV–vis spectra of (a) FeP and (b) Al-FeP in DCM.

carried out in DCM, a chlorinated solvent. To avoid the use of this solvent, EtOH was used in the present work. Mutin and Vioux [16] have previously used the alcohol route to obtain catalysts and photocatalysts, while Niederberger *et al.* [39] used chloride precursors and benzyl alcohol as solvent and oxygen donor to prepare crystalline oxide nanoparticles. In the current case, the use of EtOH offers a further advantage: the mixture of the reactants $AlCl_3$ and FeP was more homogeneous in the ethanolic reaction medium [16]. A priori, this should provide a higher number of collisions between the chemical species during the synthesis of Al-FeP.

The Soret band at 420 nm in the UV–vis spectrum of Al-FeP (Fig. 1), demonstrated that FeP was immobilized on the alumina matrix. However, no α and β bands (between 500 and 700 nm) were recorded. Ciuffi et al. [40] have reported that these bands are absent from the spectra when MePs is supported on silica, suggesting that these less intense bands were suppressed due to background noise and interference from the support. In the present case, an additional reason for the absence of these bands might be the low FeP loading on the support (9.62 mg/g), that is, FeP was diluted within the matrix, which made detection of the bands difficult. The fact that the color of the support changed from white to brown also indicated the presence of FeP on the alumina matrix.

The small red shift in the Soret band of Al-FeP as compared to the Soret band of FeP in solution suggested that the immobilization somewhat distorted the porphyrin ring, and that the FeP was probably immobilized on the surface of the solid [41].

Fig. 2 includes the TG and DTA curves for Al_2O_3, FeP, and Al-FeP. The TG curve of the Al_2O_3 sample evidenced three mass losses. The first loss, between 25 and 200 °C, was associated with an endothermic peak in the DTA curve and was assigned to the removal of the solvent and water molecules that were weakly adsorbed onto the surface of alumina. The second mass loss step occurred between 200 and 350 °C, and corresponded to the release of the solvent used during the synthesis and which had been entrapped in the matrix, together with desorption of water chemically bound to the surface of the alumina. The third mass loss, between 400 and 600 °C, was small and was associated to the pyrolysis of residual halide groups as HCl and alkoxides from the synthesis. Any mass loss above 600 °C corresponded to residual dehydration of γ-Al_2O_3 [42].

The curves obtained for FeP revealed that the organic component of the MeP decomposed in the 340–460 °C range through a strong exothermic process splitted in two steps, although only a single, continuous mass loss was recorded in the TG curve, after a first mass loss up to ca. 100 °C, which can be assigned to removal of weakly retained water molecules. The curve then showed an almost flat aspect, and the strong mass loss, probably corresponding to combustion of the organic components, started around 340 °C, ending at ca. 460 °C; above this temperature the curve was also flat. The DTA curve showed, prior to the strong exothermic effect due to combustion, some weak endothermic effects close to 90 and 230 °C, respectively. A weak exothermic effect close to 900 °C, followed by loss of mass, referred to the phase transformation.

Concerning Al-FeP, it underwent three mass loss steps, just like Al_2O_3 (actually, both curves are very similar to each other). The significant mass loss from 200 to 400 °C corresponded to pyrolysis and removal of residual groups (chlorides and alkoxides) [43], observed in the DTA curve as an endothermic event with a minimum at ca. 180 °C with a shoulder at lower temperatures. Due to the low amount of FeP supported onto the alumina matrix the effects associated to the decomposition of the porphyrin are not clearly recorded. Immobilization of MePs onto solid matrixes can change the temperature at which the porphyrin ring decomposes due to interactions between the MeP and the support. In any case, the most evident difference between the DTA curves of the alumina support and sample Al-FeP was the splitting in two effects, in the second case, of the strong endothermic effect at low temperature; this can be ascribed to an effect associated to the presence of the hydrophobic organic supported phase.

The amount of porphyrin in sample Al-FeP was determined using Eq. (2) from the mass loss between 200 and 700 °C corresponding to the removal of the alkoxide and porphyrin degradation.

$$L = \frac{W_{200-700^\circ C}}{(1 - W_{200-700^\circ C}) \cdot M} \quad (2)$$

where L is the porphyrin loading (mol porphyrin per gram of alumina), $W_{200-700\,^\circ C}$ is the mass loss corresponding to porphyrin decomposition, normalized excluding losses due to alumina dehydroxylation, water or solvent adsorbed, and alkoxide degradation; and M is the molar mass of porphyrin.

The amount of porphyrin calculated was about 10.0 mg/g of alumina, very close to the theoretical value targeted in the experiment for

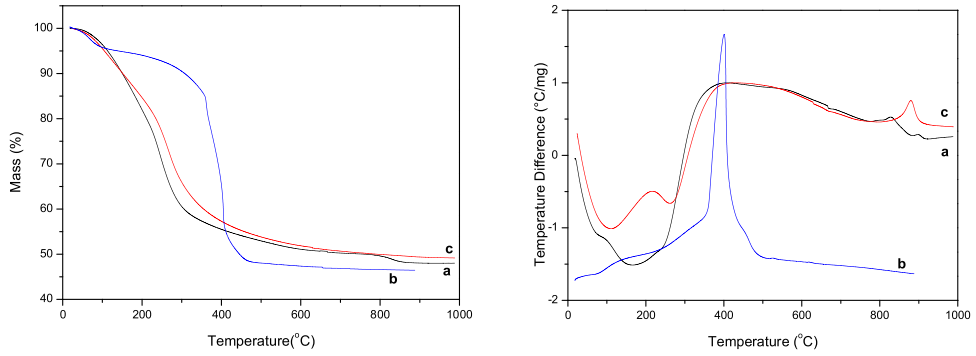

Fig. 2. TG (left) and DTA (right) curves recorded for (a) Al_2O_3, (b) FeP and (c) Al-FeP.

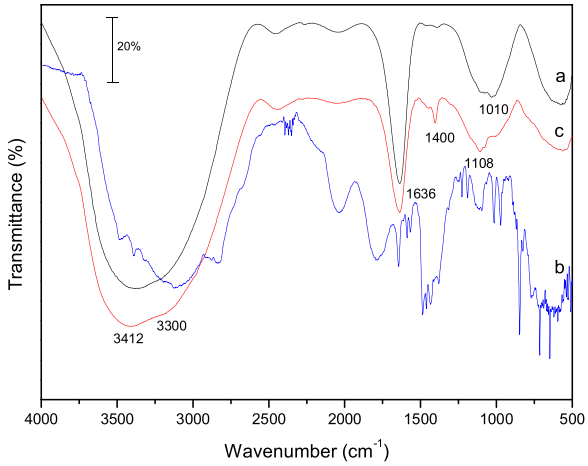

Fig. 3. Infrared absorption (FTIR) spectra of (a) Al_2O_3, (b) FeP, and (c) Al-FeP.

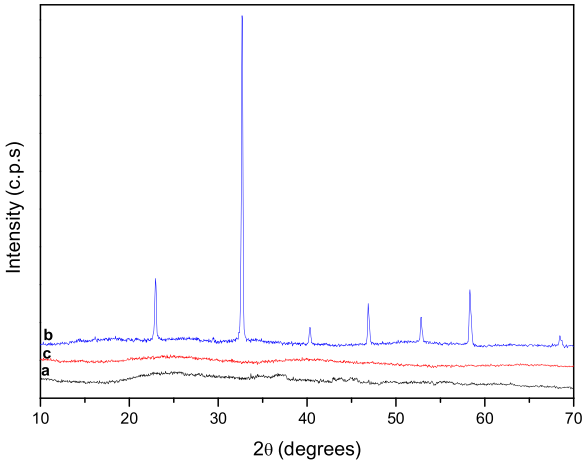

Fig. 4. PXRD diffractograms of (a) Al_2O_3, (b) FeP and (c) Al-FeP.

iron(III)-porphyrin immobilization (9.62 mg/g). The results confirmed the high affinity between the porphyrin and the alumina matrix; almost all the porphyrin used was fixed onto the alumina surface and was not leached during the exhaustive solid washing.

Fig. 3 includes the FTIR spectra of Al_2O_3, FeP and Al-FeP. The spectrum of Al_2O_3 shows an intense, very broad band centered at around 3412 cm^{-1}, due to the O—H stretching mode of hydroxyl groups in the surface of the particles and of adsorbed water molecules; the presence of molecular water was confirmed by the medium intensity band at 1636 cm^{-1}, due to the bending mode. The double band around 1000 cm^{-1} (1108 and 1010 cm^{-1}) was due to Al—OH vibrations and those at lower wavenumber to Al-O vibration modes. Concerning sample FeP, many sharp peaks were recorded, in agreement with the mostly organic nature of this compound. It is noteworthy the splitting in several components of the broad band above 2500 cm^{-1}, mostly related to different N—H vibration modes. Finally, the spectrum for sample AlFeP resembled that of Al_2O_3, probably due to the low FeP loading. The main differences were the change in the relative intensities of the two bands recorded around 1000 cm^{-1}, probably because of the formation of hydrogen bonds between the supported molecules and the surface hydroxyl groups, as well as the development of a new, weak band at ca. 1400 cm^{-1}.

Another confirmation of the presence of porphyrin in the matrix would be given by the peak corresponding to NH stretching, which usually arises in the region of 3300 cm^{-1}. This band was not present in the spectrum of FeP (Fig. 3b), maybe indicating the purity of the Fe-porphyrin, that is, that iron has completely replaced hydrogen at the center of the porphyrin ring after iron insertion into $H_2TDC(NH_2)P$. However, the presence of a broad band at 3700–3000 cm^{-1}, due to the stretching of the O—H bonds may mask the NH region, mainly considering the low loading of the porphyrin in the matrix.

Fig. 4 includes the PXRD patterns of Al_2O_3, FeP and Al-FeP. The lack of defined maxima in the diagram of the alumina support evidences its mostly amorphous nature. The diffraction halo between 20 and 30° was related to the amorphous phase of the matrix. This resulted from the dispersion halo at angles and bond distances between the basic structural units (aluminates), which destroyed the periodicity of the structure, to afford a non-crystalline material [8]. However, bulk FeP showed some sharp, well defined maxima which ascription is outside the scope of this study. Concerning sample Al-FeP, its diffraction diagram was very similar to that of Al_2O_3, due to the low FeP loading in the sample.

The specific surface areas of the materials, Table 2, were determined from the nitrogen adsorption isotherms, according to the BET method [44]. The alumina supports have high specific surface areas, 100 and 309 $m^2 g^{-1}$ for Al_2O_{3ether} and Al_2O_3, respectively, evidencing that this parameter is dependent on the synthesis method followed, and confirming the possibility of obtaining by this method materials with different morphologies, modifying the synthesis parameters. After ironporphyrin insertion, the specific surface area decreased almost to zero ($< 1\ m^2 g^{-1}$), in agreement with the incorporation of bulky molecules into porous supports, blocking the pores. With the aim of overcoming this situation, the CEC and SSA were calculated using methylene blue (MB) method (Table 2). For both solids, the CEC – and consequently the MB-measured specific surface area – increased after insertion of the porphyrin, indicating that ironporphyrin is located on the surface of the solid contributing to increase its specific surface area. The BET specific surface areas depend on the solvent used in the preparation of the materials, the solid prepared using ethanol as oxygen donor showing a larger specific surface area. These results also agreed with the data obtained by the SEM (Fig. 6) technique, the morphology of the solids also depend on the solvents used in the preparation, suggesting that the use of ethanol led to a better distribution of the ironporphyrin on the alumina matrix.

Table 2
Specific surface area (S_{BET}, accessible to N_2) and total surface area (SSA, accessible to methlylene blue) for the supports and porphyrin containing solids.

Sample	SSA (m^2/g)	S_{BET} (m^2/g)
Al_2O_3	78	309
Al-FeP	203	< 1
Al_2O_{3ether}	47	100
Al_{ether}-FeP	62	< 1

3.1. Catalytic tests

3.1.1. Epoxidation of (Z)-cyclooctene

(Z)-Cyclooctene has been used to test the activity of both homogeneous and heterogeneous catalysts. This substrate is frequently used as a model of epoxidation reactions for various reasons: (i) (Z)-cyclooctene is a suitable “diagnostic substrate” for initial studies on catalytic oxidation systems [10,45]; (ii) it generally affords (Z)-cyclooctene oxide as major product; (iii) (Z)-cyclooctene oxide is significantly more stable and easier to analyze than other epoxides [46].

First, the efficiency and stability of Al-FeP in the epoxidation of (Z)-cyclooctene by PhIO was evaluated; the results are summarized in Table 3. A control test was performed in the absence of the oxidant, not observing the formation of any product, confirming that the transference of oxygen is a concerted mechanism.

FeP and Al-FeP efficiently catalyzed the conversion of (Z)-cyclooctene to (Z)-cyclooctene epoxide. Neither aldehyde nor ketone was

Table 3
Yield of (Z)-cyclooctene oxide (%) as a function of the reaction time for the oxidation of (Z)-cyclooctene by PhIO catalyzed by FeP in homogeneous and heterogeneous conditions.[a]

Catalyst	Conversion (%)					
	2 h	4 h	24 h	48 h	TON	TOF (h^{-1})
FeP	66	69	69	69	$1.80\ 10^8$	$7.50\ 10^6$
Al-FeP	86	88	87	87	$2.27\ 10^5$	$9.46\ 10^3$

[a] Al_2O_3 was inactive.

detected after reaction in any case. In both cases, the conversion remained almost constant with time, close to 70% under homogeneous conditions and to 87% in the heterogeneous one. Al-FeP provided the best catalytic performance among the tested catalysts. Interestingly, the yield of (Z)-cyclooctene epoxide (87%) was higher than the yield of (Z)-cyclooctene epoxide obtained with FeP (70%). This is opposite to the results obtained for other heterogeneous catalysts reported in the literature [47], which generally show lower conversion than their homogeneous counterparts. The lower yield achieved with the homogeneous catalyst herein could be attributed to the low solubility of FeP in the reaction solvent. In the case of heterogeneous catalysis, immobilization of the complex may developed a larger number of active sites, and the product yield will reflect the actual capacity of FeP to oxidize substrates.

Oxidation of (Z)-cyclooctene is rather easy, and with catalysts of the type here studied the likely active catalytic species is the ferryl porphyrin π-cation radical ($Fe^{IV}(O)P^{\cdot +}$), which is greatly reactive toward the double bond of cyclic alkenes [48]. Traylor et al. [49] have described the mechanism for the epoxidation of (Z)-cyclooctene in the following steps (Fig. 5): First, FeP reacts with the oxygen donor, to generate the intermediate $Fe^{IV}(O)P^{\cdot +}$. The electron is then transferred from the π bond of the alkene substrate to the $Fe^{IV}(O)P^{\cdot +}$ intermediate, followed by the collapse of the cage and the release of an intermediate carbocation that can react according to three competitive routes: (i) nucleophilic attack of the lone pair of oxygen on the positively charged intermediate carbocation, to yield an epoxide; (ii) alkyl substitution; (iii) pinacol rearrangement, to produce an aldehyde or a ketone after cleavage of the oxygen-iron bond.

Table 4
Yield (%) of (Z)-cyclooctene oxide after 4 h reaction of (Z)-cyclooctene with PhIO catalyzed by FeP in homogeneous and heterogeneous conditions under different catalyst/substrate/PhIO molar ratios.

Catalyst	Catalyst/Substrate/PhIO molar ratio	Product yield (%)	TON	TOF (h^{-1})
Al_2O_3	1:1000:2000	0		
	1:2000:2000	0		
	1:1000:4000	0		
FeP	1:1000:2000	0		
	1:2000:2000	71	$1.85\ 10^8$	$7.71\ 10^6$
	1:1000:4000	68	$1.77\ 10^5$	$7.38\ 10^3$
Al-FeP	1:1000:2000	0		
	1:2000:2000	92	$2.40\ 10^8$	$1.00\ 10^7$
	1:1000:4000	85	$2.21\ 10^5$	$9.21\ 10^3$

The reaction was studied under different conditions, maintaining the time of reaction constant at 4 h (Table 4). On increasing the substrate ratio in the reaction medium (catalyst/substrate/PhIO molar ratio = 1:2000:2000) increased the product yield by 5%, while increasing the oxidant (PhIO) ratio (catalyst/substrate/PhIO molar ratio = 1:1000:4000) decreased the product yield by ca. 3%, which

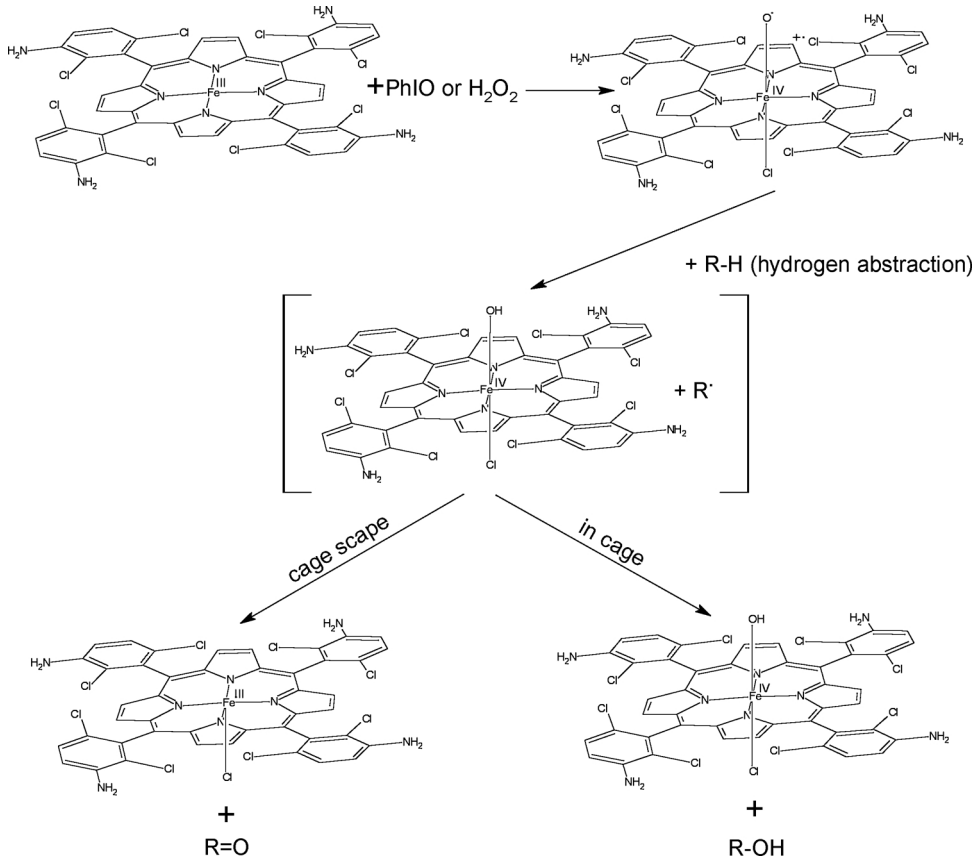

Fig. 5. Mechanism of the Fe(III) aminoporphyrin-catalysed oxidation of alkanes by PhIO and H_2O_2, showing alternative competing pathways following formation of initial solvent-caged alkyl radical and hydroxyiron(IV) aminoporphyrin (Adapted from Traylor et al. [49]).

indicated a deactivation if the catalyst intermediate by competitive reaction with PhIO or FeP [50]. Catalyst Al-FeP under heterogeneous conditions showed the best results in all tested conditions. This might have been due to the way FeP was immobilized on the support, which probably made the active catalytic complex more accessible (less hindered) for interaction with the substrate, resulting in improved catalytic performance. In addition, since the active site is more accessible, the support minimizes the occurrence of parallel competitive reactions.

The high yield obtained under homogenous conditions indicated that FeP was a good catalyst itself, but it became evident that the use of the heterogeneous catalysts led to a higher yield. The positive effect of using the heterogeneous catalyst was reinforced by its low FeP loading, the low cost of the process of inserting the FeP into the matrix, and especially on the possible reuse of the heterogeneous catalyst.

The reactions were also tested using H_2O_2 as oxidant and conducted in the presence of anhydrous (24% w/w) or aqueous (70% w/v) H_2O_2, at room temperature (27 °C) or 55 °C. 70% H_2O_2 was used on the basis of the results reported by Rinaldi et al. [51], who found that this concentration increased the lifetime and productivity of the catalysts because of a lesser decomposition of H_2O_2. In our case, this concentration would allow to achieve good yields of epoxide and lower formation of molecular oxygen. According to some authors, catalyst deactivation has prevented the use of 70% H_2O_2 in numerous reactions [28,52] but surprisingly, low yields were obtained for the reactions carried out at room temperature and 70% H_2O_2, while the yields were even lower, less than 2%, at 55 °C.

So, the presence of water with the oxidant probably deactivated FeP, and the water existing in the reaction medium may also deactivate it when supported on the alumina matrix. As an excess 70% H_2O_2 was used in the tests, the amount of water present in the reaction medium was extremely high, which may explain the results here reported. However, as observed by Rinaldi et al. [53], aqueous H_2O_2 introduced water into the reaction medium, which led to the formation of a water "layer" on the surface of the relatively hydrophilic catalyst, thereby hindering the approach of the highly hydrophobic substrate (Z)-cyclooctene. Indeed, the catalyst (Ti(IV)/SiO_2) used by Shell to produce propylene oxide cannot be used with aqueous H_2O_2 because a dense layer of water emerges on the surface of the catalyst, poisoning the Ti (IV) active site and making it inaccessible to the olefin molecule [54].

On the contrary, tests with anhydrous H_2O_2 at both temperatures afforded considerable results (Table 5). These data are promising, especially considering that mild conditions were used (non-polluting oxidant and room temperature or 55 °C). The best yields were achieved after 24 h and 48 h of reaction for the homogeneous and the heterogeneous system, respectively. The fact that the heterogeneous system required a longer reaction time to attain the same product yield than the homogeneous system was expected, as the matrix slowed down the diffusion of reactants and products to and from the active site of the substrate [10].

Anhydrous H_2O_2 increased the conversion of (Z)-cyclooctene to (Z)-cyclooctene epoxide considerably because ethyl acetate, a much less hydrophilic solvent, probably replaced water and facilitated the access of the substrate to the active site in the catalyst. Interestingly, the use of PhIO as oxidant had the opposite effect. Hence, the hydration and the hydrophilicity of the alumina surface are key factors for understanding the catalytic activity of Al-FeP: exposure to moisture under ambient conditions easily rehydrates the surface of alumina, or the reaction mixture may form a dense layer on the surface of alumina, hindering the access of the olefin to the active site.

Table 6
Yields of cyclooctene epoxide (%) as a function of the reaction time (4, 24, or 48 h) in the oxidation of (Z)-cyclooctene by anhydrous H_2O_2 catalyzed by FeP in homogeneous and heterogeneous conditions at 55 °C.[a]

Catalyst	Conversion (%)				
	4 h	24 h	48 h	TON	TOF (h^{-1})
FeP	38	43	47	$1.12\ 10^8$	$4.66\ 10^6$
Al-FeP	53	62	68	$1.61\ 10^5$	$6.71\ 10^3$

[a] $Al_2O_3$was inactive.

As for the tests involving PhIO as an oxidant, an increase in the amount of oxidant decreased the catalytic activity. As PhIO was already in excess in the reaction conditions adopted here, the reactions were repeated using H_2O_2 as oxidant instead. Table 6 shows the product yields obtained by setting up such reactions for 4, 24, and 48 h, as determined by the best values found in previous catalytic tests.

The product yields obtained in this reaction were considerably higher than those obtained previously with 70% H_2O_2. The use of a large excesss of the oxidant might have determined the low product yields, but the presence of water might have had an even more negative effect on the outcome of the reaction because of the deactivation of the catalytic matrix. The use of certain concentrations of anhydrous H_2O_2 circumvented such problems and made this oxidant an environmentally friendly alternative. These results are similar to those reported by Carvalho et al. [55] for Fe(TCPP) immobilized on kaolinite when using anhydrous H_2O_2 as oxidant and verified that the product yields resembled the product yields achieved when using PhIO as oxidant.

As FeP was active in homogeneous catalysis, the Sheldon test [54] was carried out after the catalytic reactions to determine if the catalytic activity of Al-FeP was truly heterogeneous and to prove the importance of immobilizing porphyrin in an inorganic support. This test consists of filtering off the solid after the oxidation reaction, adding an additional amount of oxidant to the resulting supernatant liquid, and allowing the oxidation reaction to proceed under the same initial conditions for further 48 h. Electronic spectra of the supernatant liquids were recorded and the Soret band was not detected in the spectra, that is, the amount of (Z)-cyclooctene epoxide in the supernatant liquid did not increase significantly as compared to the amount of epoxide formed at the end of the reaction conducted using Al-FeP as catalyst, indicating that the supported solids played an essential role in the reaction. So, the catalytic activity of Al-FeP was actually related to an heterogeneous process, confirming the importance of immobilizing the porphyrin on the inorganic support.

For comparison, the synthesis of Al-FeP was repeated in the same conditions, except that diethyl ether (ether route) was used instead of

Table 5
Yields of (Z)-cyclooctene epoxide (%) as a function of the reaction time in the oxidation of (Z)-cyclooctene by anhydrous H_2O_2 catalyzed by FeP in homogeneous and heterogeneous conditions.[a]

Catalyst	Conversion (%)											
	2 h		4 h		24 h		48 h		TON		TOF (h^{-1})	
	27 °C	55 °C	27 °C	55 °C	27 °C	55 °C	27 °C	55 °C	27 °C	55 °C	27 °C	27 °C
FeP	6	8	7	10	16	24	14	21	$4.17\ 10^7$	$6.25\ 10^4$	$1.73\ 10^6$	$3.60\ 10^3$
Al-FeP	7	10	6	11	8	18	9	20	$2.08\ 10^4$	$4.69\ 10^4$	$1.17\ 10^3$	$1.95\ 10^3$

[a] Al_2O_3 was inactive.

ethanol (alcohol route) [11], obtaining the material designated Al_{ether}-FeP. Mutin and Debecker observed that the use of different oxygen donors (e.g., alcohol or ether) led to distinct NHGR mechanisms, producing materials with specific characteristics [19]. For this reason, the ether route was explored to prepare the catalyst in an attempt to explain the catalytic behavior of Al_{ether}-FeP as compared to the catalytic behavior of Al-FeP in oxidation reactions where hydrogen peroxide was the oxidant. Although the ether route followed by Lima et al. [11] was efficient to obtain catalysts for the oxidation of hydrocarbons, the structural character of the matrixes generated by this route produced fragile materials after thermal treatment, with the presence of acidic sites that deactivated hydrogen peroxide when it was used as the oxidant in oxidative processes catalyzed by Al_{ether}-FeP.

Indeed, catalyst Al_{ether}-FeP afforded 28% epoxide yield in the oxidation of (Z)-cyclooctene by iodosylbenzene, as compared to 53% achieved with catalyst Al-FeP. When catalyst Al_{ether}-FeP was used in the oxidation of (Z)-cyclooctene by hydrogen peroxide, no epoxide was formed, which indicated that the different preparation routes gave products with specific, different characteristics. In general, aluminas have been reported as efficient catalysts for the oxidation of olefins [56]. Their non-toxicity can be combined with the advantages of environmentally friendly oxidants, like hydrogen peroxide. Therefore, we attempted to understand the mechanisms involved in the two different preparation routes.

Three parameters are crucial for the catalytic activity of heterogeneous solids in the oxidation of alkenes: (1) the presence of Brönsted and Lewis acidic sites, (2) a hydrophilic surface, and (3) the texture of the catalyst (morphology). In this sense, the acidity sites in the solids Al_2O_3, Al_2O_{3ether}, Al-FeP and Al_{ether}-FeP were analyzed by vibrational spectroscopy. The areas of the bands arising from the interaction between pyridine and alumina or between alumina-porphyrin were used to calculate the surface concentration of Brönsted and Lewis sites [57]. This analysis revealed bands at 1535, 1485 and 1450 cm^{-1}, which corresponded to Brönsted sites, interaction between Brönsted and Lewis sites, and Lewis sites or hydrogen bonds, respectively [35,57–59]. The estimated concentrations of Brönsted (q_B) and Lewis (q_L) and $q_{B/L}$ sites are given in Table 7.

The data showed that both Al_2O_3 and Al_2O_{3ether} had structural hydroxyls. As expected, the ether route resulted in complete condensation of the alkoxide generated in situ, so Al_2O_{3ether} had not surface hydroxyl groups (or only a minor concentration): the ether route consisted in a direct route that produced Al-O-Al and alkyl halide. Debecker and Mutin [19] highlighted that the ether route provides oxo bridges in the first step after in situ formation of alkoxide groups and their reaction with chloride groups, Eq. (3). In a second step, ether reacts with chloride groups according to Eq. (4):

$$M–Cl + M–OR \rightarrow M–O–M + R–Cl \quad (3)$$

$$M–Cl + ROR \rightarrow M–OR + R–Cl \quad (4)$$

where M–Cl = metal chloride, M–OR = alkoxide, M–O–M = oxo bridge, and R–Cl = alkyl chloride.

The results obtained here agreed with the expected properties of the solids considering the synthesis routes followed. The ether route did not generate hydroxyl groups, Eqs. (3) and (4). The presence of small amounts of Brönsted sites was a result of the exposure of the samples to ambient air. As for the alcohol route, the use of a primary alcohol such as ethanol should not produce hydroxyl groups, either Eq. (5). However, the hydrochloric acid generated during the reaction may have promoted secondary reactions producing hydroxyl groups, responsible for acidic sites.

$$M–Cl + ROH \rightarrow M–OR + H–Cl \quad (5)$$

Several authors [60,61], have reported that the hydroxyl groups of alumina perform essential roles in catalysis. Schuchardt and Rinaldi [60] studied the epoxidation of cis-cyclooctene by hydrogen peroxide and observed that hydrogen peroxide was probably activated through reaction with weak acidic sites (Al—OH) on the surface of alumina, to form hydroperoxide groups that could transfer oxygen to the alkene.

Hydrophilicity is essential to ensure rapid reaction between alumina and hydrogen peroxide to form surface Al − OOH groups. Thus, thermogravimetry was used to measure the different concentrations of water molecules on the surface of samples Al_2O_3, Al_2O_{3ether}, Al-FeP, and Al_{ether}-FeP. First, the samples were dried at 100 °C and then they were submitted to thermal analyses to determine the amount of water that was adsorbed onto the solids. The results are summarized in Table 8.

Once again, it was confirmed that Al_2O_{3ether} contained fewer hydroxyl groups and therefore had less affinity for water molecules as compared to Al_2O_3, which was more hydrophilic. However, when FeP was supported on the alumina matrixes, the hydrophilic character of the solids was reversed, and Al_{ether}-FeP was more hydrophilic than Al-FeP.

The presence of water can deactivate the heterogeneous catalyst because the water molecules can coordinate to the active site of the FeP. Further investigations on the hydrophilicity of Al-FeP catalysts were therefore necessary because this is an essential parameter considering that the use of hydrogen peroxide as an oxidant requires an aqueous medium.

On the basis of the results concerning acidic sites and hydrophilicity, it became clear that the FeP molecule was bound to Al_2O_3 and to Al_2O_{3ether} in different ways. Interaction between the matrix and pyridine groups on the FeP generated acidic sites, which indicated that the active catalytic sites (FeP) were on the surface of Al-FeP, whereas FeP was entrapped into the pores of Al_{ether}-FeP. This justified the different results concerning acidic sites, catalytic activity toward alkenes, and hydrophilicity obtained for Al-FeP and Al_{ether}-FeP.

When examining the morphology of the materials (Fig. 6), it was confirmed that the use of different solvents led to the formation of materials with distinct morphologies, indicating that FeP was located at different positions of the alumina matrix in Al-FeP and in Al_{ether}-FeP.

Table 7
Brönsted and Lewis acidity of alumina and alumina-porphyrin materials.

Brönsted and Lewis sites	Concentration (μmol g^{-1})			
	Al_2O_3	Al-FeP	Al_2O_{3ether}	Al_{ether}-FeP
q_B (1535 cm^{-1})	31.03	24.59	2.32	28.60
$q_{B/L}$ (1485 cm^{-1})	1.33	1.33	1.33	1.33
q_L (1450 cm^{-1})	7.72	2.20	13.01	23.14

Table 8
Amount of water (% of the mass of the solid) removed between 25–900 °C of alumina and alumina-porphyrin materials.

Catalyst	W (%)
Al_2O_3	2.63
Al-FeP	2.38
Al_2O_{3ether}	2.49
Al_{ether}-FeP	2.80

3.1.2. Oxidation of cyclohexane

To confirm the versatility of FeP and Al-FeP systems, they were evaluated for the oxidation of saturated hydrocarbons, which are less reactive than the unsaturated ones. Cyclohexane was chosen as a saturated substrate because it is relatively inert and has been extensively used in the literature [8,10,62]. This substrate provides information not only on the catalytic efficiency, but also on the selectivity of a given catalyst to a particular product.

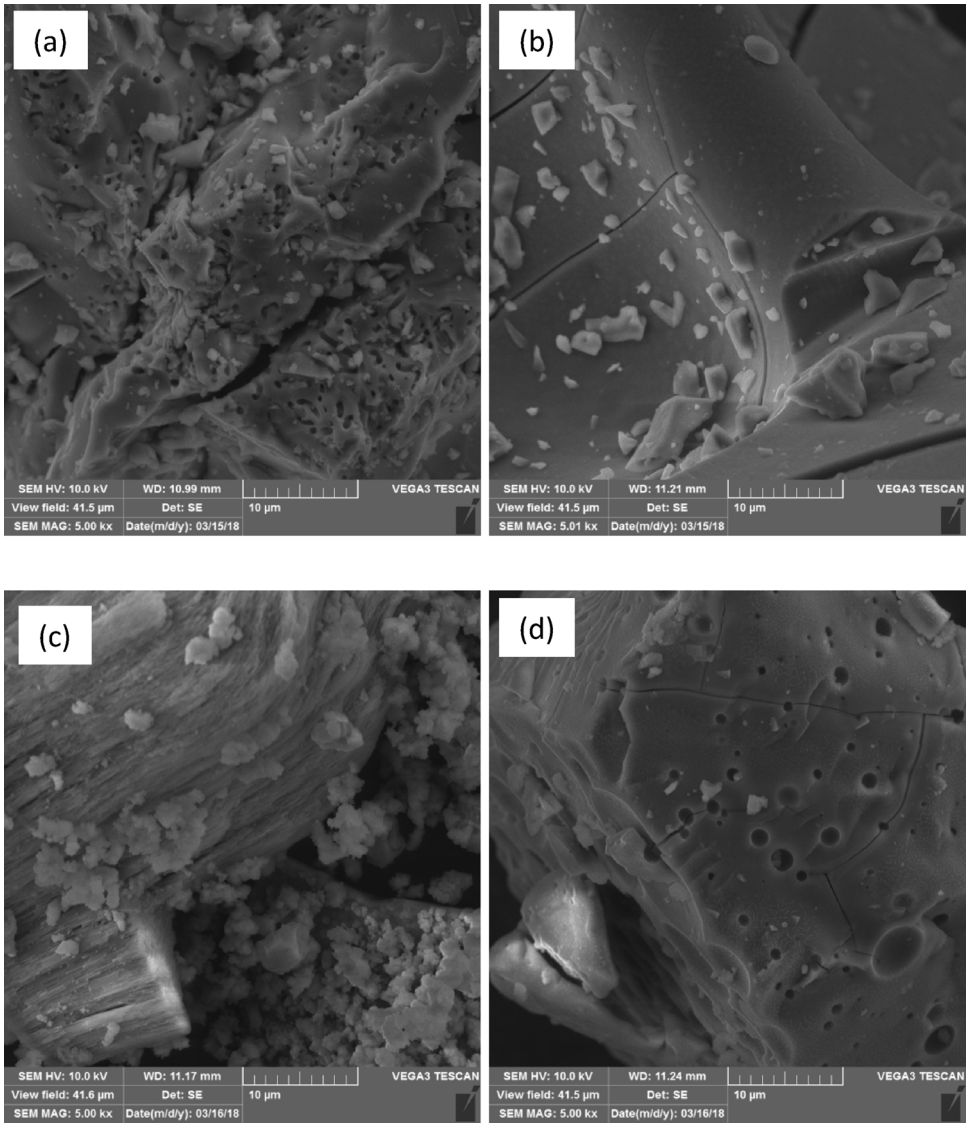

Fig. 6. Scanning electron microscopy (SEM) of (a) Al_2O_3, (b) Al-FeP, (c) Al_2O_{3ether} and (d) Al $_{ether}$-FeP.

Table 9
Yields of cyclohexanol (OL) and cyclohexanone (ONE) as a function of time in the oxidation of cyclohexane by PhIO catalyzed by FeP in homogeneous and heterogeneous conditions.[a]

Catalyst	Product Yield (%)									
	2 h		4 h		24 h		48 h			
	OL	ONE	OL	ONE	OL	ONE	OL	ONE	TON	TOF (h^{-1})
FeP	–	–	–	12	–	17	–	17	$1.12\ 10^8$	$4.67\ 10^6$
Al-FeP	–	–	–	19	–	20	–	20	$4.25\ 10^7$	$1.77\ 10^6$

[a] Al_2O_3 was inactive.

Table 9 lists the results obtained in the oxidation of cyclohexane. All the materials selectively catalyzed the oxidation to cyclohexanone (formation of cyclohexanol was not observed in any case), which was produced in yields higher than those reported by the industry [63], wherein the oxidation of cyclohexane gives a mixture of cyclohexanone/cyclohexanol (KA-oil) using toxic oxidants and homogeneous catalysts. As in the case of the oxidation of (Z)-cyclooctene, Al-FeP showed a higher catalytic efficiency than FeP, suggesting that the support enhanced the catalytic activity of the FeP complex. All the tested materials showed unusual selectivity for cyclohexanone, whereas catalytic MeP systems are generally selective for cyclohexanol [8,21,64,65]. For instance, Machado et al. [8] reported 20% and 14% cyclohexanol yield with homogeneous Fe(TDFSPP) and Fe(TDFSPP) immobilized on kaolinite triethanolamine (loading = 10.4×10^{-6} mol/g). Other authors [65–67] have described yields of 55% or even 70% for cyclohexanol, but cyclohexanone was also formed, lowering the selectivity of the systems.

The active catalytic species in oxidation reactions catalyzed by FeP systems is iron(IV)–oxo porphyrin π-radical cations, $Fe^{IV}(O)P^{\cdot+}$ [48]. Mechanistic studies involving FePs have suggested that, after formation of the active catalytic species, interaction of FeP with PhIO may generate a new intermediate species within a solvent cage, [Fe^{IV} − OH + R], where R refers to the substrate. Production of cyclohexanol and/or cyclohexanone will depend directly upon the formation of this new species. If the OH fragment binds to the substrate radical, cyclohexanol is formed. However, if this recombination does not occur rapidly, the substrate radical species escapes from the solvent cage, to give other products such as cyclohexanone [8,68]. An important feature of such caged radical species is the competition between the in-cage radical recombination and the diffusive cage escape.

The use of anhydrous H_2O_2 as oxidant afforded lower product yields (≤1%) as compared to PhIO as oxidant. Indeed, gas bubbles (oxygen)

Table 10
Conversion of cyclohexanone to ε-caprolactone (%) via Baeyer-Villiger oxidation with H_2O_2 70% as oxidant, catalyzed by FeP in homogeneous and heterogeneous conditions at 27 °C, at a catalyst/substrate/oxidant molar ratio of 1:3000:15,000.[a]

Catalyst	Conversion (%)					
	2 h	4 h	24 h	48 h	TON	TOF (h^{-1})
FeP	–	1	4	7	$1.00\ 10^7$	$4.17\ 10^5$
Al-FeP	–	2	2	4	$5.01\ 10^3$	$2.09\ 10^2$

[a] $Al_2O_3$was inactive.

evolved along the reaction, which pointed to decomposition of H_2O_2 and showed that the reaction was inefficient.

The tests performed at room temperature were ineffective, so they were conducted at 55 °C. According to the results reported by Carvalho et al. [55]. systems operating below 20 °C rapidly lose activity and selectivity. Temperatures above 40 °C lead to evaporation of cyclohexane. Therefore, the ratio between the reactants was altered to improve the results.

3.1.3. Baeyer–Villiger (BV) oxidation

Heterogeneous MeP systems can mimic the action of enzymes during the BV reaction; these MeP systems can catalyze the transformation of linear and cyclic ketones to their corresponding esters and lactones [10,55], generally using peroxyacids as oxidants. However, on an industrial scale peroxyacids generate large amounts of acidic wastes, which causes additional costs related to recycling and regeneration of the active oxidizing species [28]. Various catalysts have been tested for BV reactions, but few of them have allowed the use of clean oxidants like H_2O_2 [69,70].

An efficient catalyst for BV oxidation should be able to increase the nucleophilicity of the peroxide. This activation should boost the oxidative activity of the peroxide toward electrophiles such as the carbonyl group. As Al-FeP can potentially mimic the cytochrome P-450 monooxygenases, its efficiency was evaluated in the BV oxidation of cyclohexanone to the corresponding lactone.

Table 10 lists the product yields obtained in the BV oxidation of cyclohexanone by H_2O_2 70% catalyzed by FeP in homogeneous and heterogeneous conditions at 27 °C, calculated on the basis of the consumed oxidant.

The hydrophobicity of the catalyst is an important parameter to be considered when aqueous H_2O_2 is used as an oxidant. Deactivation of catalysts in the presence of water is one of the major drawbacks for the use of this oxidant in numerous reactions [51]. In the current case, deactivation of Al-FeP could occur via the formation of a dense layer of water on the surface of the alumina matrix, which would hinder the access of the substrate to the active catalytic site. In addition, water existing in the reaction medium could hydrolyze the ε-caprolactone formed. These events would account for the low product yields obtained.

Even though water could promote parallel reactions and deactivate the surface of the alumina matrix [28], the presence of a small amount of water in the reaction medium is necessary to activate the surface of alumina by rehydration, regenerating Brönsted acid sites (Al—OH). This should form surface Al—OOH species that transfer oxygen species to the substrate. Another reason for the low product yields could be the relatively low temperature used during the catalytic tests (less than 90 °C) [28], which prevented water to be removed from the reaction medium and thus decreased the conversion.

On the basis of literature data [28,55], further tests were conducted at 80 °C using anhydrous H_2O_2 as oxidant in an attempt to improve the yield to ε-caprolactone (Table 11).

The catalysts acted selectively and efficiently in the BV oxidation, to produce the lactone. The homogeneous catalyst showed the best results in the tests using anhydrous H_2O_2. After 48 h of reaction, similar results were obtained for the supported Al-FeP catalyst.

The reaction temperature was a key factor. Reactions conducted at room temperature led to lower conversions because water could not be removed from the reaction medium and deactivated the catalyst. Reactions conducted above 95 °C caused higher release of O_2 via decomposition of H_2O_2 in the reaction medium, leaving a small amount of oxidant available for the reaction and decreasing conversion. A temperature higher than 27 °C and lower than 95 °C, such as 80 °C, should avoid the loss of reagent [28].

According to Lamas et al. [71], the addition of benzonitrile to the solvent aids oxygen transfer. Reactions conducted in the absence of this compound do not produce ε-caprolactone. Therefore, it can be inferred that the BV reaction involves two stages: First, H_2O_2 attacks the Brönsted sites on the surface of the catalyst, to form hydroperoxide species, which is followed by the attack of benzonitrile to produce an intermediate. Then, there is a nucleophilic attack on the carbonyl group of cyclohexanone, to generate the Criegee adduct, and subsequent rearrangement of the intermediate, to give an ester and a benzamide species. This mechanism is summarized in Fig. 7.

In the case of the electrophilic activation of the substrate (cyclohexanone), Brönsted or Lewis acids can activate the carbonyl group, increasing the polarizability of the C═O double bond and facilitating the nucleophilic attack by H_2O_2.

3.2. Oxidation of organic substrates in the presence of a radical trap

The reaction mechanisms described for catalytic systems involving metal ions such as iron and oxidants like H_2O_2 have been a matter of controversy in the literature because free radicals can be formed in the reaction medium. Several mechanisms have been proposed for such systems, some of which include active radical species as the oxidizing agent [72,73]. To find out whether the reaction mechanism followed by the Al-FeP involves a radical path, the oxidation of (Z)-cyclooctene was carried out using the well-known radical scavenger hydroquinone [74,75] and using anhydrous H_2O_2 as oxidant. The reactions were carried out at 55 °C, for 48 h, at a catalyst/substrate/oxidant molar ratio of 1:1000:2000, under magnetic stirring. The presence of hydroquinone

Table 11
Conversion of cyclohexanone to ε-caprolactone (%) via Baeyer-Villiger oxidation with 70% H_2O_2 (Aq) or anhydrous H_2O_2 (Anh) as oxidants, catalyzed by FeP in homogeneous and heterogeneous conditions at 80 °C, at a catalyst/substrate/oxidant molar ratio of 1:3000:15,000.[a]

Catalyst	Reaction time (h)											
	2		4		24		48		TON		TOF (h^{-1})	
	Aq	Anh	Aq	Anh	Aq	Anh	Aq	Anh	Aq	Anh	Aq	Anh
FeP	–	–	14	34	17	40	17	42	$3.97\ 10^7$	$9.35\ 10^7$	$1.65\ 10^6$	$3.90\ 10^6$
Al-FeP	–	–	21	33	23	36	25	41	$5.37\ 10^4$	$8.41\ 10^4$	$2.24\ 10^3$	$3.50\ 10^5$

[a] Al_2O_3 was inactive.

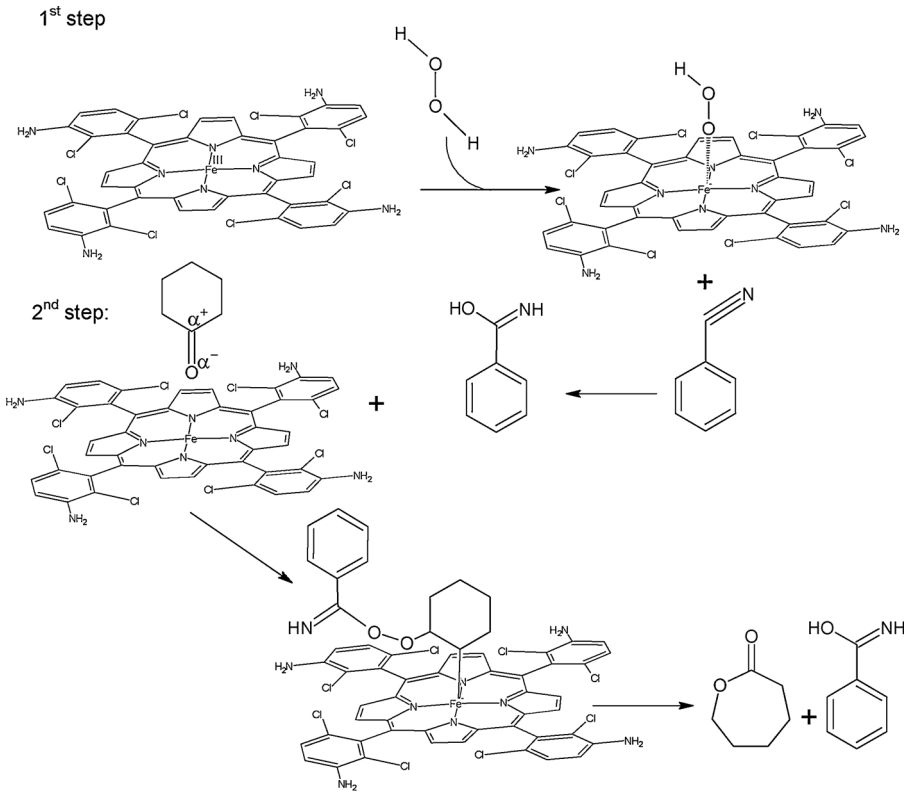

Fig. 7. Baeyer-Villiger proposed mechanism for cyclohexanone oxidation in the presence of benzonitrile, using iron(III) aminoporphyrin as catalyst (Adapted from Llamas et al. [71]).

increased the conversion to (Z)-cyclooctene epoxide from 68% to 90%, indicating that a free radical mechanism also held during the epoxidation—there was a competition between the active catalytic species and the radical species, as observed by Ciuffi et al. [45] for Ni-aluminosilicate catalyst.

On the contrary, the presence of the radical trap did not modify the catalytic efficiency of Al-FeP in the BV reaction, suggesting that this reaction did not involve free radical species. In fact, this reaction involves two steps [71]: In the first step, H_2O_2 attacks the cationic Fe species, coordinated to an axial chloro ligand, in the porphyrin ring, to form the hydroxide species, which in turn attacks benzonitrile and generates the peroxycarboximidic intermediate. In the second step, Fe (from ironporphyrin) behaves as a Lewis acid site and interacts with the carbonyl oxygen, to produce the lactone and regenerating the catalyst.

The fact that this catalytic process was not governed by a radical mechanism is advantageous because non-radical mechanisms culminate in higher selectivity [76,77] so Al-FeP can mimic biological enzymes, such as cytochrome P-450.

3.3. Reuse

The possibility of reusing supported catalysts in further reaction cycles is one of the most important benefits of heterogeneous catalysis, especially in the case of transition metal complexes and MeP systems, among others, which are often expensive or difficult to prepare. Here, the high efficiency and stability of Al-FeP was verified for catalyst reuse. To this end, the catalyst was separated from the reaction mixture after each experiment by simple filtration and dried before using it again in a subsequent run.

Table 12 shows the catalytic results regarding the reuse of Al-FeP at catalyst/substrate/anhydrous H_2O_2 molar ratios of 1:1000:2000 and 1:3000:15,000. Al-FeP was used in three consecutive runs without any significant decrease in activity; only a small reduction in catalytic performance was observed in the first reuse, followed by an increase in the conversion values in the second reuse. There was no noticeable leaching of the solid catalyst during the washing procedure, so the lower conversion in the first reuse could not be attributed to loss of the solid catalytic species. The increased conversion values in the second and third reuse may have been due to the higher availability of active sites, which had been probably blocked prior to the tests.

Table 12
Recycling of Al-FeP in the epoxidation of (Z)-cyclooctene by anhydrous H_2O_2 for 24 h, at 55 °C, at different catalyst/substrate/oxidant molar ratios.

Molar ratio	Conversion of (Z)-cyclooctene (%)			
	Test	1st reuse	2nd reuse	3rd reuse
1:1000:2000	68	66	71	73
1:3000:15,000	20	18	22	23

The catalytic behavior of the Al-FeP solid combines the advantage of fast and efficient catalysis compared to the homogeneous catalytic systems, with the possibility of reuse (characteristic of heterogeneous catalysts).

4. Conclusions

The process used for the immobilization of porphyrins proved to be an efficient route in the preparation of Al-FeP catalysts. The solids synthesized showed catalytic activity for the oxidation of different organic substrates by both iodosilbenzene and hydrogen peroxide. The best yields for catalytic epoxidation of cyclooctene for the supported catalyst were 85–92%, using PhIO as oxidant and up to 68% using anhydrous H_2O_2 as the oxidant, under mild temperatures. An interesting selectivity for cyclohexanone was observed in the oxidation reactions of cyclohexane, which made very important to use the porphyrin $FeTDCNH_2$ as the biomimetic catalyst for oxidation reactions.

The reaction temperature was a parameter that influenced the catalytic activity, since the reactions with heating presented higher yields, facilitating the diffusion of the reagents and products.

There are no papers in the literature reporting the catalytic behavior of this ironporphyrin in the oxidation reactions of cyclooctene and cyclohexane and in Baeyer-Villeger reaction. The results obtained are very promising as a heterogeneous catalyst presents advantages when compared to the homogeneous one, and it can be easily reused, making it economically viable.

Acknowledgements

The authors thank to the Spain– Brazil Interuniversity Cooperation Grant, jointly funded by the Spanish Ministry of Education, Science and Sports (PHBP14/00003) and CAPES (317/15) and a Cooperation Grant jointly financed from Universidad de Salamanca and FAPESP (2016/50322-2).

The Brazilian group acknowledges the support from the Brazilian research funding agencies Fundação de Amparo à Pesquisa do Estado de São Paulo (FAPESP) (311767/2015-0, 2012/08618-0, 2013/19523-3 and 2016/01501-1), Coordenação de Aperfeiçoamento de Pessoal de Nível Superior (CAPES) and Conselho Nacional de Desenvolvimento Científico e Tecnológico (CNPq).

References

[1] P. Barbaro, F. Liguori, Heterogenized Homogeneous Catalysts for Fine Chemicals Production, first ed., Springer, Netherlands, 2010.
[2] P.T. Anastas, M.M. Kirchhoff, T.C. Williamson, Appl. Catal. Gen. 221 (2001) 3–13.
[3] T. Miyao, S. Sakurabayashi, W. Shen, K. Higashiyama, M. Watanabe, Catal. Commun. 58 (2015) 93–96.
[4] W. Zhang, P. Jiang, Y. Wang, J. Zhang, J. Zheng, P. Zhang, Chem. Eng. J. 257 (2014) 28–35.
[5] X. Yu, A. Manthiram, Appl. Catal. B: Environ. 165 (2015) 63–67.
[6] A.B. McQuarters, M.W. Wolf, A.P. Hunt, N. Lehnert, Angew. Chem. Int. Ed. 53 (2014) 4750–4752.
[7] P.R. Ortiz de Montellano, Cytochrome P450 — Structure, Mechanism, and Biochemistry, third ed., Springer, US, 2005.
[8] G.S. Machado, K.A.D. de F. Castro, O.J. de Lima, E.J. Nassar, K.J. Ciuffi, S. Nakagaki, Colloids Surf. Physicochem. Eng. Aspects 349 (2009) 162–169.
[9] Y. Iamamoto, Y.M. Idemori, S. Nakagaki, J. Mol. Catal. Chem. 99 (1995) 187–193.
[10] N. Bizaia, E.H. de Faria, G.P. Ricci, P.S. Calefi, E.J. Nassar, K.A.D.F. Castro, S. Nakagaki, K.J. Ciuffi, R. Trujillano, M.A. Vicente, A. Gil, S.A. Korili, ACS Appl. Mater. Interfaces 1 (2009) 2667–2678.
[11] O.J. de Lima, D.P. de Aguirre, D.C. de Oliveira, M.A. da Silva, C. Mello, C.A.P. Leite, H.C. Sacco, K.J. Ciuffi, J. Mater. Chem. 11 (2001) 2476–2481.
[12] S. Nakagaki, G.K.B. Ferreira, A.L. Marçal, K.J. Ciuffi, Curr. Org. Synth. 11 (2014) 67–88.
[13] S. Nakagaki, G. Machado, M. Halma, A.Ados S. Marangon, K.A.D. de F. Castro, N. Mattoso, F. Wypych, J. Catal. 242 (2006) 110–117.
[14] C. Sanchez, J. Livage, M. Henry, F. Babonneau, J. Non-Cryst. Solids 100 (1988) 65–76.
[15] C.J. Brinker, G.W. Scherer, Sol-Gel Science, The Physics and Chemistry of Sol-Gel Processing, first ed., Academic Press, Boston, 2013.
[16] P.H. Mutin, A. Vioux, Chem. Mater. 21 (2009) 582–596.
[17] V. Smeets, L. Ben Mustapha, J. Schnee, E.M. Gaigneaux, D.P. Debecker, Mol. Catal. 452 (2018) 123–128.
[18] P.H. Mutin, A. Vioux, J. Mater. Chem. A 1 (2013) 11504–11512.
[19] D.P. Debecker, P. Hubert Mutin, Chem. Soc. Rev. 41 (2012) 3624–3650.
[20] B.L. Caetano, L.A. Rocha, E. Molina, Z.N. Rocha, G. Ricci, P.S. Calefi, O.J. de Lima, C. Mello, E.J. Nassar, K.J. Ciuffi, Appl. Catal. Gen. 311 (2006) 122–134.
[21] G.P. Ricci, Z.N. Rocha, S. Nakagaki, K.A.D.F. Castro, A.E.M. Crotti, P.S. Calefi, E.J. Nassar, K.J. Ciuffi, Appl. Catal. A: Gen. 389 (2010) 147–154.
[22] O.J. de Lima, A.T. Papacídero, L.A. Rocha, H.C. Sacco, E.J. Nassar, K.J. Ciuffi, L.A. Bueno, Y. Messaddeq, S.J. Ribeiro, Mater. Charact. 50 (2003) 101–108.
[23] M. Rico-Santacruz, E. Serrano, G. Marcì, E.I. García-López, J. García-Martínez, Chem.—Eur. J. 21 (2015) 18338–18344.
[24] J. Zhu, J. Yang, Z.-F. Bian, J. Ren, Y.-M. Liu, Y. Cao, H.-X. Li, H.-Y. He, K.-N. Fan, Appl. Catal. B: Environ. 76 (2007) 82–91.
[25] T.C.O. Mac Leod, D.F.C. Guedes, M.R. Lelo, R.A. Rocha, B.L. Caetano, K.J. Ciuffi, M.D. Assis, J. Mol. Catal. Chem. 259 (2006) 319–327.
[26] J.M.A. Caiut, S. Nakagaki, O.J.D. Lima, C. Mello, C.A.P. Leite, E.J. Nassar, K.J. Ciuffi, H.C. Sacco, J. Sol-Gel Sci. Technol. 28 (2003) 57–64.
[27] H. Saltzman, J.G. Sharefkin, Org. Synth. 43 (1963) 60.
[28] R.A. Steffen, S. Teixeira, J. Sepulveda, R. Rinaldi, U. Schuchardt, J. Mol. Catal. Chem. 287 (2008) 41–44.
[29] D.C. de Oliveira, H.C. Sacco, O.R. Nascimento, Y. Iamamoto, K.J. Ciuffi, J. Non-Cryst. Solids 284 (2001) 27–33.
[30] J.S. Lindsey, I.C. Schreiman, H.C. Hsu, P.C. Kearney, J. Org. Chem. 52 (1987) 827–836.
[31] A.D. Adler, F.R. Longo, W. Shergalis, J. Am. Chem. Soc. 86 (1964) 3145–3149.
[32] A. Vioux, Chem. Mater. 9 (1997) 2292–2299.
[33] G. Orsini, V. Tricoli, J. Mater. Chem. 21 (2011) 14530–14542.
[34] T. Barzetti, E. Selli, D. Moscotti, L. Forni, J. Chem. Soc. Faraday Trans. 92 (1996) 1401–1407.
[35] C.A. Emeis, J. Catal. 141 (1993) 347–354.
[36] A.C. da Silva, K.J. Ciuffi, M.J. dos Reis, P.S. Calefi, E.H. de Faria, Appl. Clay Sci. 126 (2016) 251–258.
[37] L. Marçal, D. Faria, E.H.M. Saltarelli, P.S. Calefi, E.J. Nassar, K.J. Ciuffi, R. Trujillano, M.A. Vicente, S.A. Korili, A. Gil, Ind. Eng. Chem. Res. 50 (2011) 239–246.
[38] L.M.L. da Silva, Fda C. Silva, A.L. de Carvalho, L. Marçal, M. Saltarelli, E.H. De Faria, L.A. Rocha, P.S. Calefi, K.J. Ciuffi, E.J. Nassar, Int. Sch. Res. Not. 2012 (2012) 1–6.
[39] M. Niederberger, M.H. Bartl, G.D. Stucky, J. Am. Chem. Soc. 124 (2002) 13642–13643.
[40] K.J. Ciuffi, H.C. Sacco, J.C. Biazzotto, E.A. Vidoto, O.R. Nascimento, C.A. Leite, O.A. Serra, Y. Iamamoto, J. Non-Cryst. Solids 273 (2000) 100–108.
[41] G.S. Machado, K.A.D. de Freitas Castro, F. Wypych, S. Nakagaki, J. Mol. Catal. Chem. 283 (2008) 99–107.
[42] R. Rinaldi, U. Schuchardt, J. Catal. 236 (2005) 335.
[43] S. Acosta, R.J.P. Corriu, D. Leclercq, P. Lefèvre, P.H. Mutin, A. Vioux, J. Non-Cryst. Solids 170 (1994) 234–345.
[44] S. Brunauer, P.H. Emmett, E. Teller, J. Am. Chem. Soc. 60 (1938) 309–319, https://doi.org/10.1021/ja01269a023.
[45] K.J. Ciuffi, E.J. Nassar, L.A. Rocha, Z.N. da Rocha, S. Nakagaki, G. Mata, R. Trujillano, M.A. Vicente, S.A. Korili, A. Gil, Appl. Catal. Gen. 319 (2007) 153–162.
[46] K.A.D.F. Castro, M. Halma, G.S. Machado, G.P. Ricci, G.M. Ucoski, K.J. Ciuffi, S. Nakagaki, J. Braz. Chem. Soc. 21 (2010) 1329–1340.
[47] S. Nakagaki, K.A.D.F. Castro, G.M. Ucoski, M. Halma, V. Prévot, C. Foranob, F. Wypych, J. Braz. Chem. Soc. 25 (2014) 2329–2338.
[48] J.T. Groves, J. Inorg. Biochem. 100 (2006) 434–447.
[49] T.G. Traylor, C. Kim, J.L. Richards, F. Xu, C.L. Perrin, J. Am. Chem. Soc. 117 (1995) 3468–3474.
[50] G.M. Ucoski, K.A.D. de F. Castro, K.J. Ciuffi, G.P. Ricci, J.A. Marques, F.S. Nunes, S. Nakagaki, Appl. Catal. Gen. 404 (2011) 120–128.
[51] R. Rinaldi, F.Y. Fujiwara, U. Schuchardt, Catal. Commun. 5 (2004) 333–337.
[52] G.-J. ten Brink, I.W.C.E. Arends, R.A. Sheldon, Chem. Rev. 104 (2004) 4105–4124.
[53] R. Rinaldi, F. Fujiwara, U. Schuchardt, J. Catal. 245 (2007) 456–465.
[54] R. Sheldon, I.W.C.E. Arends, Appl. Catal. Gen. 212 (2001) 175–187.
[55] A.L. de Carvalho, B.F. Ferreira, C.H.G. Martins, E.J. Nassar, S. Nakagaki, G.S. Machado, V. Rives, R. Trujillano, M.A. Vicente, A. Gil, S.A. Korili, E.H. de Faria, K.J. Ciuffi, J. Phys. Chem. C 118 (2014) 24562–24574.
[56] N.A. Stephenson, A.T. Bell, J. Mol. Catal. Chem. 275 (2007) 54–62.
[57] F.J. del Rey-Perez-Caballero, G. Poncelet, Microporous Mesoporous Mater. 37 (2000) 313–327.
[58] B. González, R. Trujillano, M.A. Vicente, V. Rives, E.H. de Faria, K.J. Ciuffi, S.A. Korili, A. Gil, Environ. Chem. 14 (2017) 267–278.
[59] E.P. Parry, J. Catal. 2 (1963) 371–379.
[60] R. Rinaldi, U. Schuchardt, J. Catal. 227 (2004) 109–116.
[61] G. Busca, Catal. Today 226 (2014) 2–13.
[62] B. Gao, Y. Chen, Q. Lei, J. Incl. Phenom. Macrocycl. Chem. 74 (2012) 455–465.
[63] U. Schuchardt, D. Cardoso, R. Sercheli, R. Pereira, R.S. da Cruz, M.C. Guerreiro, D. Mandelli, E.V. Spinacé, E.L. Pires, Appl. Catal. A: Gen. 211 (2001) 1–17.
[64] A.L. Faria, M. Leod, V.P. Barros, M.D. Assis, J. Braz. Chem. Soc. 20 (2009) 895–906.
[65] M. Halma, F. Wypych, S.M. Drechsel, S. Nakagaki, J. Porphyr. Phthalocyanines 06 (2002) 502–513.
[66] S. Nakagaki, M. Halma, A. Bail, G.G.C. Arízaga, F. Wypych, J. Colloid Interface Sci. 281 (2005) 417–423.
[67] M. Halma, A. Bail, F. Wypych, S. Nakagaki, J. Mol. Catal. Chem. 243 (2006) 44–51.
[68] X. Huang, J.T. Groves, J. Biol. Inorg. Chem. 22 (2017) 185–207.
[69] X. Li, R. Cao, Q. Lin, Catal. Commun. 63 (2015) 79–83.
[70] J.P. Mehta, D.K. Parmar, H.D. Nakum, D.R. Godhani, N.C. Desai, Microporous Mesoporous Mater. 247 (2017) 198–207.
[71] R. Llamas, C. Jiménez-Sanchidrián, J.R. Ruiz, Tetrahedron 63 (2007) 1435–1439.
[72] R. Buffon, U. Schuchardt, J. Braz. Chem. Soc. 14 (2003) 347–353.
[73] B.P.C. Hereijgers, R.F. Parton, B.M. Weckhuysen, Catal. Sci. Technol. 2 (5) (2012) 951–960.
[74] M.K. Tse, M. Klawonn, S. Bhor, C. Döbler, G. Anilkumar, H. Hugl, W. Mägerlein, M. Beller, Org. Lett. 7 (2005) 987–990.
[75] B.B. Wentzel, P.L. Alsters, M.C. Feiters, R.J.M. Nolte, J. Org. Chem. 69 (2004) 3453–3464.
[76] H.J.H. Fenton, J. Chem. Soc. Trans. 65 (1894) 899–910.
[77] F. Gozzo, J. Mol. Catal. Chem. 171 (2001) 1–2.